ChemPubSoc Europe

DOI: 10.1002/cctc.201501243

CHEMCATCHEM Full Papers

Palladium Supported on Nanodiamonds as an Efficient Catalyst for the Hydrogenating Deamination of Benzonitrile and Related Compounds

Neeraj Gupta, Yuxiao Ding, Zhenbao Feng, and Dangsheng Su*[a]

Palladium nanoparticles were successfully prepared on a nanodiamond (ND) support and used for the hydrogenating deamination of benzonitrile, aromatic imines, and amines for the first time. The developed methodology was further used for the in situ conversion of aldehydes into hydrocarbons, including a biomass-derived model compound. The activity of the catalyst was compared with palladium supported on activated carbon (AC) under identical conditions and the performance of Pd/ND was found to be superior to Pd/AC. The origin of the difference in the catalytic performance was considered. Finally, an attempt has been made to understand the mechanism through the identification of the side products by GCMS analysis.

1. Introduction

Removal of a particular functional group is of the utmost importance to some synthetic organic processes such as decyanation,[1] deamination,[2] and hydrodeoxygenation,[3] which are frequently used during fine chemical and drug synthesis. Decyanation processes generally involve the loss of a cyanide group,[1] resulting in carbon loss. Chemical processes involving the conversion of cyanides to alkanes with the retention of the carbon atom are rarely reported in literature, but developing such a method could provide the dual benefit of decyanation and alkylation. Deamination of aromatic amines is generally achieved by a two-step process involving diazotization followed by reduction with different reductants. Also, examples of one-pot conversions of aromatic amines to alkanes are very few[4] in the literature. For the removal of an aldehyde group from organic compounds, rhodium compounds[5] have derived considerable attention since the use of Wilkinson's catalyst[6] for this particular reaction. Beside Rh, other catalytic systems involving Ir,[7] Ru,[8] and Pd[9] compounds have also been studied. More recently, Maiti et al.[10] have used $Pd(OAc)_2$ for the decarbonylation of aldehydes. The major drawback of these reactions is the loss of a carbon atom during the transformations, which makes them less atom efficient. To attain better atom efficiency, a two-step approach involving reduction of the aldehyde followed by hydrodeoxygenation[11] was employed. This also suffers from low yields and contamination of the final product with the alcoholic intermediate. Therefore, a single-step process providing high yields of alkanes without carbon loss and without involving an alcoholic intermediate would be highly beneficial. Moreover, most of the reported processes involve homogeneous catalytic systems in which catalyst separation always remains a major challenge. Thus, developing the analogous processes with the use of a heterogeneous catalytic system is highly beneficial.

Nanodiamonds (ND), one of the recently explored nanocarbon materials, have many attractive features and a wide range of applications[12] in various fields such as the development of magnetic sensors, biomedical imaging, drug delivery, and chemical transformations. Recently, a number of reviews[13] have been published to highlight the importance of nanodiamonds in medicinal, chemical, and related fields. Metal nanoparticles (NPs) supported on different supports,[14] including carbon,[15] have remarkable properties and have been used in various chemical transformations.[16] Metal nanoparticles on nanodiamonds have been recently used for developing nanomedicines,[17] as electrocatalyst in fuel cells,[18] and in the oxygen reduction reaction.[19] Palladium NPs supported on nanodiamonds exhibit enhanced activity towards the hydrogenation[20] of the C=C and C≡C bonds. They were also used in the hydrogenation[21] of cyclohexene, allyl alcohol, nitrobenzene, azomethines, allyl alcohol, and simultaneously for the reductive amination of propanal[22] with 4-aminobenzoic acid. Careful study of these literature reports indicate that NDs are a good support for transition metals such as Pd. Metal NPs supported on NDs are resistant to agglomeration during reactions under a hydrogen atmosphere. Alekseev et al.[23] have reported that hydrogen reduction at 600 °C did not increase the Pd particle size on the ND surface, whereas it increased almost ten times upon analogous treatment on activated carbon (AC). It is generally hypothesized that the high activity of metals supported on NDs is due to surface ordering and the almost complete absence of micropores.

[a] Dr. N. Gupta, Dr. Y. Ding, Dr. Z. Feng, Prof. D. Su
Catalysis Division
Shenyang National Laboratory for Materials Science
Institute of Metal Research
Chinese Academy of Sciences
Shenyang, 110016 (P.R. China)
E-mail: dssu@imr.ac.cn

Supporting Information for this article is available on the WWW under http://dx.doi.org/10.1002/cctc.201501243.

Based on our continuing efforts to explore carbon materials[24] for different chemical transformations and the exceptionally good properties of nanodiamond supports in comparison to activated carbon, we present herein a new methodology for the hydrogenating deamination reaction of benzonitrile and analogous compounds by using palladium nanoparticles supported on nanodiamonds. The developed catalyst provides the double benefit of decyanation and deamination and can also indirectly substitute the hydrodeoxygenation process that is used for the removal of aldehydic groups in organic molecules. First, it is used for the reductive cleavage of the –C≡N bond in benzonitrile and later also for the cleavage of the carbon–nitrogen bond in aromatic imines and amines. The methodology was linked to the removal of aldehydic groups in aromatic aldehydes and used for the conversion of model biomass-derived compounds.

2. Results and Discussion

2.1. Catalyst characterization

We first prepared palladium nanoparticles supported on nanodiamonds (Pd/ND) and a detailed description of the catalyst preparation can be found in the Experimental Section. Commercially available nanodiamonds from Beijing Grish Hitech Co. (China) were used in the study. The surface morphology and nature of the materials was first characterized by scanning transmission electron microscopy (STEM). From Figure 1a, it is clear that the Pd nanoparticles were uniformly distributed on the surface of the NDs. Figure 1b shows that the nanoparticles (bright contrast) are decorated on NDs and are well exposed. Both the Pd nanoparticles and NDs exhibited good crystallinity; a lattice spacing of 0.22 nm in the magnified STEM image (Figure 1c) of a Pd nanoparticle could be assigned to the (111) crystal plane of metallic Pd. We further performed a fast Fourier-transform (FFT) on the micrograph, and indexed the bright spots in the pattern (Figure 1d) to be the {111}, {002}, and {111} planes of a cubic Pd crystal, as labeled in the image. The signature of Pd was confirmed by X-ray photoelectron spectroscopy (XPS) at ~335 eV and the elemental contents of Pd/ND and Pd/AC are summarized in Table 1. Deconvolution on the high-resolution Pd 3d feature (Figure S1 in the Supporting Information) suggests that Pd^0 (334.9 eV for $3d_{5/2}$) and Pd^{2+} (336.5 eV) species exist in a ratio of approximately 5:1; this was found to be similar for both Pd/ND and Pd/AC.

We further performed N_2 adsorption studies to determine the surface area of the catalysts (Table 1). For Pd/ND, the Brunauer–Emmett–Teller (BET) surface area was calculated to be 309 $m^2 g^{-1}$, which is not much different from that of the pure NDs (313 $m^2 g^{-1}$). On the other hand, the BET surface area of AC was reduced quite considerably after introduction of Pd nanoparticles. This likely suggests that the Pd nanoparticles grew on the surface of NDs as exposed nanoparticles (with stacking pores of average size ~20 nm), whereas the nanoparticles grew in the micropores of AC (<2 nm), clogging the open micropores, and resulting in a reduced accessible area. Growth of the metal nanoparticles on the relatively larger stacking pores of ND or on the macropores of AC may not result in any influence on the activity as the active metal particles may remain accessible in these cases.

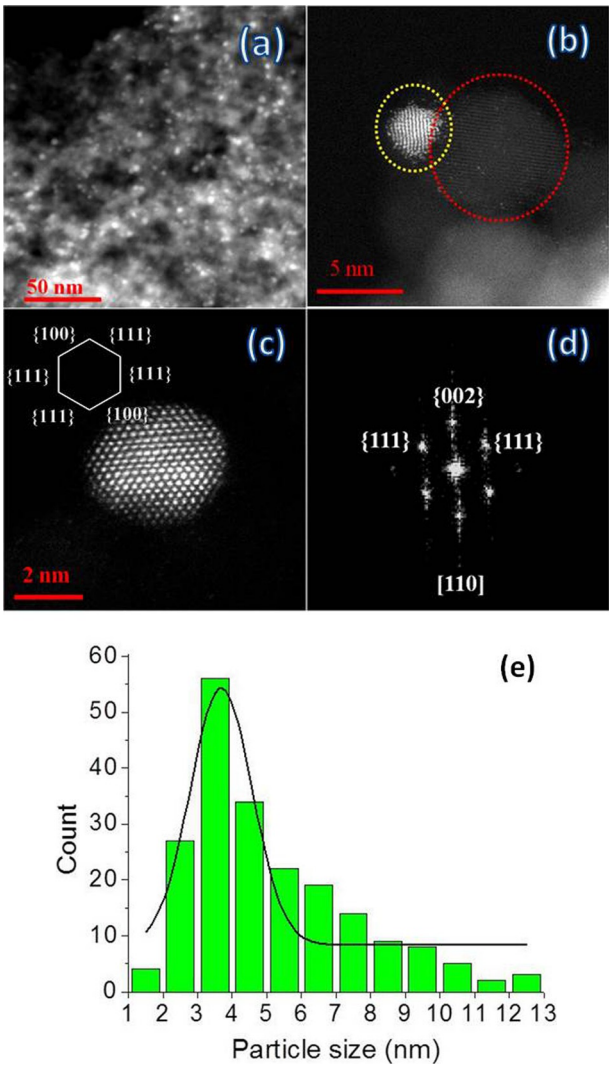

Figure 1. STEM images and particle size distribution histogram of Pd/ND: a) STEM image of Pd/ND; b) Pd nanoparticle on the surface of ND; c) magnified STEM image of Pd nanoparticle with schematic representation of its crystal structure; d) fast Fourier transform pattern of image (c); e) particle size distribution histogram of palladium nanoparticles on Pd/ND.

Table 1. Specific surface area measurements and XPS analysis of Pd/ND and Pd/AC.

BET surface area [$m^2 g^{-1}$]				XPS analysis		
ND	Pd/ND	AC	Pd/AC		Pd/ND [At%]	Pd/AC [At%]
313	309	1201	930	carbon	91.22	94.73
–	–	–	–	oxygen	8.6	4.99
–	–	–	–	Pd 3d	0.19	0.28

2.2. Hydrogenating deamination (HDA) of benzonitrile by Pd/ND and the synthetic utility

Catalytic reduction of benzonitrile (BN) is one of the very important reactions used for the preparation of amines on an industrial scale. The reduction of BN involves multiple hydrogenated or semi-hydrogenated products/intermediates. Dibenzylamine (DBA) and benzylamine (BA) are the major products reported for the reduction of benzonitrile using Pd supported on activated carbon (Pd/AC).[25] We started by testing the efficiency of Pd/ND towards this reaction. It was found that Pd/ND can reduce BN to BA, but DBA was also formed as a side product. The highest selectivity of BA obtained was 85% at a low temperature and high pressure (Table 2, entry 7) without the use of any additives such as ammonia[26] or acid.[27] The BA selectivity decreases with rising temperature or with lowering pressure. Thus, high pressure and low temperature seem to favor the formation of BA and we do not observe high selectivity of BA in non-polar cyclohexane or in polar EtOH/H_2O mixtures. From these studies, Pd/ND favors formation of BA over DBA at pressures above 1 MPa and at comparatively low temperatures (below 100 °C) in comparison to those reported in the literature,[25] where temperatures around 100 °C or above are reported. Surprisingly, 100% conversion of BN was observed at 0.5 MPa at 120 °C and no trace of BA or DBA were observed. The obtained product was confirmed as toluene (yield, 99%) by GC analysis.

The deaminated product toluene could be generated either from BN or from its hydrogenation product BA.[25] To determine which, we analyzed the reaction mixture at different time intervals (Figure S4 in the Supporting Information) under identical conditions (120 °C and 0.5 MPa H_2 pressure). It was interesting to note that toluene was the major product noticed at different stages of the reaction in THF and that very small amounts of BA were detected during the initial stage only (2% after 1 h). No trace of DBA was observed at any stage of the reaction and the selectivity of toluene reached a maximum of 99% after 6 h. These results clearly indicate that the deaminated product was directly formed from benzonitrile without involving amine formation. After the optimization process, Pd/ND was further tested for the hydrogenating deamination of related molecules (Table 3). Nicotinonitrile and related pyridine-containing compounds are abundant in natural products and hence applying this catalyst for the removal of the cyanide group in these molecules will open new doors for related reactions during natural product syntheses. Such strategies are also valuable while studying the structure–activity relationships of pharmaceutically active compounds. Therefore, reductive cleavage of 3-cyanopyridine was performed, which afforded 72% yield of 3-methyl pyridine (Table 3, entry 4). Non-aromatic substrates such as octanonitrile did not undergo any conversion. Thus, the presence of the aromatic ring is essential for the reaction. Also, if a carbon–nitrogen bond is present in the aromatic ring as well as in the side chain, the one that is adjacent to the stable aromatic ring is cleaved preferably at relatively high temperatures. Furthermore, imines and amines are classes of organic compounds that contain carbon–nitrogen double and single bonds and hence the same process can be applied for the hydrogenating cleavage of the carbon–nitrogen bonds in these molecules. To test this, the reductive cleavage of the –C=N– bond in benzyl phenylmethanimine (Table 3, entry 7) and benzylamine (Table 3, entry 10) have been carried out. Here, we also observed that the aromatic substrate BA was converted to toluene, but *n*-octylamine did not show any conversion. This again confirmed our earlier observation that the aromatic ring is essential for the conversion.

The end products of the hydrogenating deamination reaction are aromatic alkanes; one of the objectives of biomass conversion is to get alkanes from naturally abundant aldehydes. Lignin and sugar derivatives generally provide aromatic aldehydes[28] from naturally abundant resources. The hydrogenating deamination of imine derivatives performed in the previous stage serves as a link to correlate aldehydes with alkane formation through this route and hence the developed catalyst could be used for the conversion of aromatic aldehydes to alkanes. Therefore, we first converted benzaldehyde into an imine by reacting it with BA in the presence of activated

Table 2. BN reduction with Pd/ND under different conditions.

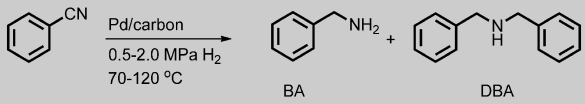

Entry	Catalyst	Solvent	Pressure [MPa]	T [°C]	t [h]	BN Conversion [%]	Yield [%] BA	DBA
1	Pd/ND	CH	1	70	3	98	60	33
2	Pd/ND	EtOH	1	70	3	93	52	2
3	Pd/ND	EtOH/H_2O[a]	1	70	3	90	49	29
4	Pd/ND	MeOH	1	70	3	72	23	3
5	Pd/ND	THF	1	70	3	4	0	0
6	Pd/ND	EtOH	1.6	70	1	55	27	T[b]
7	Pd/ND	THF	2	70	2	33	28	1
8	Pd/ND	THF	2	100	3	76	61	4
9	Pd/ND	THF	0.5	100	3	67	14	2
10	Pd/ND	THF	0.5	120	6	100	0	0
11	Pd/ND	THF	0	120	6	10	0	0
12	Pd/ND-NH_3[c]	THF	0.5	120	6	59	18	23
13	Pd/AC[d]	MeOH	1	70	3	74	2	1
14	Pd/AC	THF	1	70	3	5	0	T[b]
15	Pd/AC	CH	1	70	3	26	11	15
16	Pd/AC	EtOH	1	70	3	90	6	3
17	Pd/AC	EtOH	1.6	70	3	50	5	3
18	Pd/AC	THF	0.5	100	3	35	8	2
19	Pd/AC	THF	0.5	120	6	66	0	T[b]
20	ND	THF	0.5	120	6	0	0	0

Reaction conditions: 100 mg of benzonitrile, 10 mg of catalyst, 10 mL of solvent under the reported time, temperature (internal), and pressure. CH = cyclohexane, THF = tetrahydrofuran, EtOH = ethanol, and MeOH = methanol. [a] De-mineralized water (25 μL) was added to the reaction mixture. [b] Trace [T] quantities detected were less than 1 mg. [c] 40 mg of the catalyst was used. [d] The side product detected during the reduction of benzonitrile in all cases was toluene.

Table 3. Reductive deamination of nitriles, imines and amines.

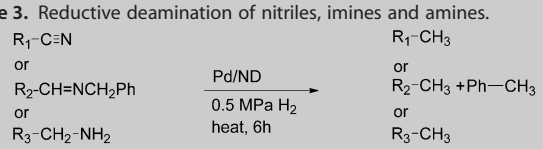

Entry	Substrate	T [°C]	Product yield [%]
1	R^1 = phenyl	120	99
2	R^1 = 3-pyridyl	120	5
3	R^1 = 3-pyridyl	150	26
4	R^1 = 3-pyridyl	175	72
5	R^1 = heptyl	120	0
6	R^2 = phenyl	120	58[a]
7	R^2 = phenyl	175	94[a]
8	R^2 = 4-methylphenyl	175	97
9	R^3 = phenyl	120	71
10	R^3 = phenyl	150	99
11	R^3 = phenyl	175	99
12	R^3 = heptyl	120	0

Reaction conditions: 100 mg of substrate, 10 mg of Pd/ND, 10 mL THF under 0.5 MPa hydrogen pressure at specified temperature (internal). [a] Total amount of toluene was divided by two.

molecular sieves (4 Å) and its complete conversion was ensured before addition of the catalyst. The yield of toluene was found to be 98% (Table 4) at 150 °C, indicating that the catalyst is effective for the direct conversion of aromatic aldehydes to hydrocarbons. It was then tested on biomass-derived model molecules to test its efficiency for biomass conversion. Vanillin, containing –OH, $-OCH_3$, and –CHO groups on the benzene ring was chosen for the study as a model compound. These groups are in abundance in lignin-derived molecules. Interestingly, excellent yield of 2-methoxy-4-methyl phenol during the conversion of vanillin was obtained under similar reaction conditions. In this process, no decrease in the number of carbon atoms occurs; hence, it is good for attaining high atom efficiencies. Furthermore, the use of this catalyst for converting furan-derived compounds did not prove beneficial.

Table 4. Conversion of aldehydes into hydrocarbons, including biomass-derived compounds.

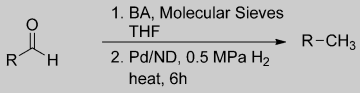

Entry	Aldehyde	Product	T [°C]	Yield [%]
1	benzaldehyde	toluene[a]	150	98
2	vanillin	2-methoxy-4-methyl phenol	150	97
3	furfural	2-methyl furan	150	2
4	furfural	2-methyl furan	110[b]	0

Reaction conditions: 100 mg aldehyde, 1 mol equiv. BA, 50 mg molecular sieves, 10 mL THF at 60 °C for 2.5 h, then 10 mg of Pd/ND was added and the mixture heated under 0.5 MPa hydrogen pressure. The internal temperature of the reaction mixture is reported. [a] Total amount of toluene was divided by two. [b] Reaction was performed for two hours.

2.3. Surface chemistry of the carbon support

The reduction of BN by Pd/AC was also performed by adopting similar conditions (Table 2) and the catalyst (Pd/AC) was prepared from commercially available activated carbon (see the Supporting Information). It was found that the performance of Pd/ND was better than that of Pd/AC and Pd/ND can perform the reduction of BN to BA at much lower temperature. Reduction of BN by Pd/AC is mostly performed at temperatures above 100 °C as shown by earlier literature reports. Also, under similar conditions (Table 2, entries 10 and 19), the performance of Pd/AC in the hydrogenating deamination reaction was lower in comparison to Pd/ND. Previous literature reports have also shown that metal NPs supported on nanodiamonds showed improved activity in comparison to activated carbon during the hydrodechlorination reaction of hexachlorobenzene[29] and 2,4,8-trichlorodibenzofuran.[30] On this basis, we could hypothesize that the difference in the activity may arise from the following factors. The active metal on the catalyst support may show different activity towards hydrogen owing to different crystal structures, different surface distribution, and different interactions with the support. At the same time, the different surface nature of the support may also influence the reaction. The presence or absence of micropores and the different concentration of surface functional groups might affect the access to the active sites and adsorption of reactant/intermediates on the catalyst surface.

As the Pd nanoparticles have identical natures on both of the catalyst surfaces (Figure 1, Figures S2 and S3 in the Supporting Information), the contribution from different crystal structures or distributions of metal is negated. Also, by comparing the HR-TEM images of the Pd/ND (Figure 1b) and Pd/AC (Figure S2), it seems that the metal particles on the surface of Pd/ND are well exposed in comparison to Pd/AC, which may further increase access to the active sites. Kachevskii et al.[31] observed significant differences in the temperature-programmed reduction spectra of PdO/ND and PdO/AC. The peak of reduction of PdO on NDs shifted towards lower temperatures in comparison to PdO/AC. The difference was explained based on the easy reduction of PdO on the nanodiamond surface owing to weak interactions between the metal and support and the unblocking effect offered by the support, which increases the availability of the metal towards hydrogen. As our catalytic system matches very closely to the reported work, hence a similar effect may also operate during the reduction of benzonitrile. It is well-known fact that surfaces of nanodiamonds have very ordered structure and have almost a complete absence of micropores[12] in comparison to activated carbon. We have observed a decrease in surface area during the preparation of Pd/AC (Table 1), which may possibly be explained by the blockage of the micropores by Pd nanoparticles, which may further decrease access to the active sites.

To understand the difference in the distribution of surface functional groups, the high-resolution O1s spectra (XPS) of both the catalysts were further investigated (Figure 2). The Pd/ND surface was rich in overall oxygen content (8.6%) in comparison to Pd/AC (4.99%). Furthermore, the surface of the

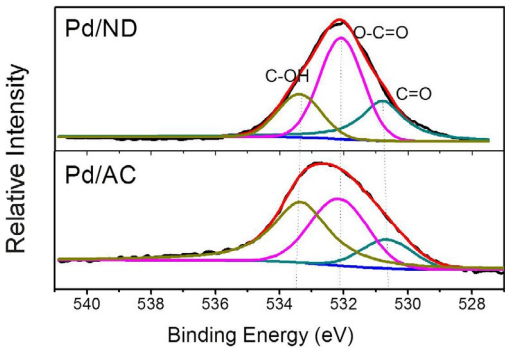

Figure 2. O 1s XPS spectra of Pd/ND and Pd/AC.

nanodiamond was rich in O–C=O functionality in comparison to activated carbon, which is also reported in the literature.[12] To see if these acidic groups might influence the reaction, we first prepared Pd/ND-NH_3 (see the Experimental Section). An ion-exchange reaction of acidic functional groups with aqueous ammonia solution can help to remove the acidic protons from the catalyst surface. Then, we performed the reductive cleavage of the CN bond in benzonitrile by the optimized process and observed the yield and selectivity of toluene (Table 2, entry 12). As expected, the yield and selectivity of toluene was drastically decreased even when using four times of the catalyst amount compare with Pd/ND. This indicated that the acidic groups on the carbon surface might play a role during the hydrogenating deamination reaction.

To see if the adsorption of the reactant and/or the intermediates/products was responsible for the different behavior, we studied the adsorption of benzonitrile, benzylamine, and toluene on the nanodiamond and activated carbon surfaces. BN, BA, and toluene (100 mg) were added to THF (25 mL) followed by the addition of ND or AC (100 mg each). GC analysis was performed after 24 h to determine the quantities of the respective compounds remaining in the solution. No significant difference in the adsorbed quantities of toluene and BN was observed, but there was a significant difference in the adsorption of BA: 30 mg of BA was adsorbed on AC and only 5 mg was adsorbed on ND. Because benzylamine formation is not observed during the hydrogenating deamination reaction (Figure S4), its differential adsorption also did not seem to affect the deamination reaction. However, it can certainly affect the BA or DBA formation during the hydrogenation of BN at low temperature and high pressure (Table 2). Because BA exhibited more adsorption on the activated carbon surface, it may show a greater tendency to stay on its surface along with the other intermediates. When BA is formed at lower temperature (Table 2, entry 7) and high pressure on a nanodiamond surface, most likely it leaves the surface and therefore its further deamination and side reaction with possible imine intermediates is minimized.

2.4. Possible mechanism for the hydrogenating deamination of BN

To investigate the possible pathway of the reaction, the different side products were identified by the GCMS analysis of the reaction mixture (Figure S5 in the Supporting Information). In addition to toluene (the main product of the hydrogenation deamination of benzonitrile), the other products identified in trace amounts are cyclohexanecarbonitrile and benzene. No trace of benzylamine or dibenzylamine was detected during the analysis. Direct conversion of BN to toluene was also observed during the optimization studies (Figure S4). Therefore, benzonitrile directly undergoes hydrogenating deamination to form toluene without involving the BA intermediate. In addition, cleavage of BA was not facile in comparison to BN reduction under identical conditions (Table 3, entry 9) and the similar observation has been reported previously.[26] This also rules out the possibility of fast cleavage of the carbon–nitrogen bond in BA on the catalyst surface.

The formation of cyclohexanecarbonitrile in trace amounts was clear evidence for the activation of the aromatic ring by Pd, which was responsible for the ring reduction. Therefore, it is probable that the π-electron cloud of the aromatic ring is interacting with Pd during the reaction to form an intermediate that gives toluene as the final product (Figure S6 in the Supporting Information). This fact is further supported by the reluctance of octanonitrile and *n*-octylamine (which do not contain aromatic rings in their structures) towards hydrogenating deamination under similar conditions (Table 3, entries 5 and 12). Therefore, the catalyst most probably activates the aromatic ring in BN and cleaves the CN bond in the intermediate (Figure S6). Cleavage of the CN bond is favored in comparison to the carbon–carbon bond in the intermediate, which favors the deaminated product and therefore toluene is the major product in comparison to benzene. We have also observed that toluene formation is minimized if the acidic groups on the surface are exchanged with aqueous ammonia solution (Section 2.3).

Based upon these facts, a mechanism is proposed for the reaction (Figure 3). The reaction starts with the interaction of benzonitrile with the palladium nanoparticles, where the ring is probably activated by Pd and similar interactions could possibly be involved with the CN functional group. Well exposed Pd nanoparticles on the surface serve as active sites for hydrogen absorption. Activation of the aromatic ring then may lead to the hydrogenation of the –CN functional group and acidic groups present on the surface might assist in the cleavage of the carbon–nitrogen bond, leading to the deaminated product. The high temperature and low pressure during this conversion further seems to assist this cleavage (Figure 3), which seems to operate in a synchronized way. If this arrangement is disturbed, this ultimately disturbs the selectivity of the deamination reaction. The fact is manifested by the reactions at 100 and 120 °C (Table 2, entries 8–10): at 100 °C, BA formation was observed at a high pressure of 2 MPa, whereas at 0.5 MPa, HDA is favored at 120 °C in comparison to 100 °C.

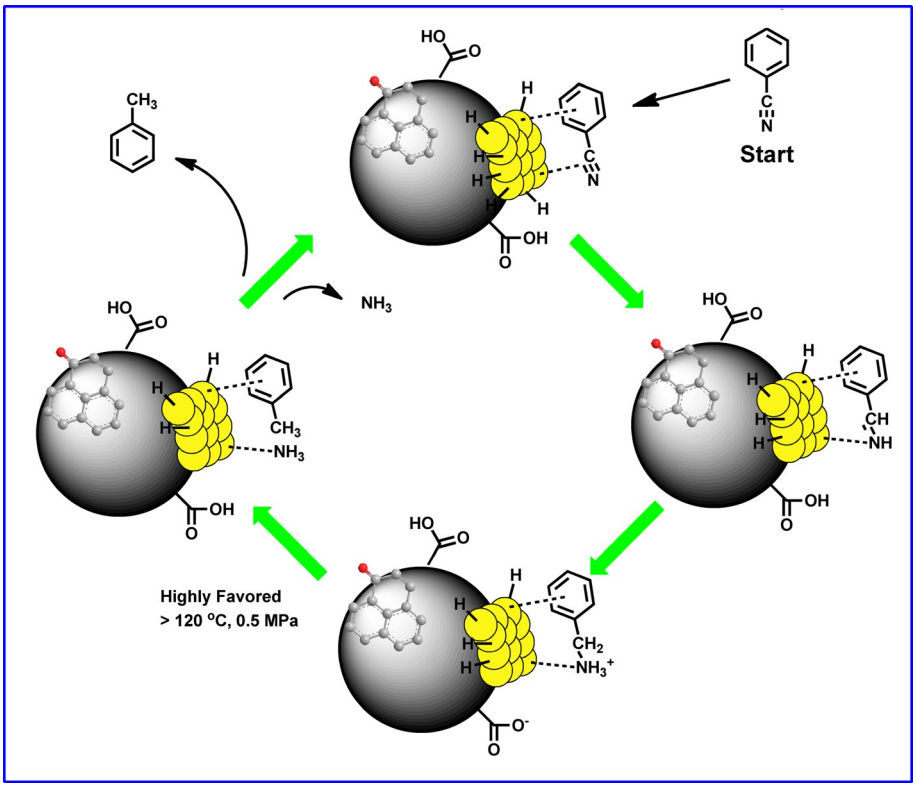

Figure 3. Plausible reaction mechanism for the HDA reaction by Pd/ND.

3. Conclusions

We have prepared palladium nanoparticles on nanodiamond surfaces and applied them in the hydrogenating deamination reaction of nitriles, imines, and amines for the first time. It was found that Pd/ND possesses excellent activity towards hydrogenating deamination and can be used for the removal of cyanide, imine, amine, and aldehydic groups in organic molecules with very high selectivity towards deaminated product. No traces of other hydrogenating products, such as analogous amines (BA or DBA) were observed during the conversion. The presence of uniformly distributed acidic sites with good exposure of palladium nanoparticles are the key factors that result in the good activity of the Pd/ND catalyst. The catalyst can also be applied for biomass conversion by the removal of aldehyde groups in lignin-derived compounds, which potentially provides an alternative chemical path for biomass utilization.

4. Experimental Section

4.1. Preparation of catalyst

Commercially available nanodiamonds (500 mg) were added to dilute HNO_3 (25 mL) at pH 3 and stirred at room temperature (25 °C) followed by the addition of $Pd(NO_3)_2$ solution in demineralized water (1 mL, 0.069 M). The contents were stirred at the same temperature for 2 h and then water was evaporated under reduced pressure at 50 °C. The obtained mass was kept overnight to ensure evaporation of trace amounts of water and then transferred to a quartz crucible. It was then heated in a fixed-bed quartz glass tube reactor at 150 °C for 2 h under an argon gas flow (100 mL min^{-1}). Finally, the temperature was increased to 300 °C and sample was heated under a flow of hydrogen gas (80 mL min^{-1}) for 2 h and then slowly cooled to room temperature. The solid obtained is labeled as Pd/ND; it was stored at room temperature and used as such in the experiments. Pd/AC was also prepared by following the identical procedure. Pd/ND-NH_3 was prepared from Pd/ND. Pd/ND (50 mg) was treated with aqueous ammonia solution at 50 °C for 2 h in an autoclave. The air in the autoclave was replaced with hydrogen gas to prevent Pd oxidation. The autoclave was cooled to room temperature and the material was dried under vacuum at 40 °C for 16 h.

4.2. Standard procedure for the reduction of benzonitrile

Tetrahydrofuran (10 mL) was added to the Teflon vessel in the autoclave reactor (100 mL) followed by the addition of benzonitrile (100 mg) and Pd/ND (10 mg). The reactor was closed and then flushed with nitrogen and hydrogen gas to displace air. Care was taken to check the hydrogen level in the surroundings by using a hydrogen gas sensor (Caution: hydrogen is flammable). Finally, the hydrogen gas was inserted at the desired pressure of 0.5 MPa and the contents were heated at 120 °C for 6 h (Table 2). The pressure of the autoclave rose from 0.5 MPa to 1.1 MPa at equilibrium. Finally, the mixture was cooled to room temperature and the pressure of the autoclave was released slowly. The reaction mixture was analyzed by gas chromatography and the yield of the product was reported by comparison with the standard calibration curve of toluene. Other products, such as 3-cyanopyridine, benzylamine, and imines, were also reductively cleaved by a similar procedure. The yields in these cases were calculated by comparison with the standard calibration curve of the specific products.

4.3. Standard procedure for the in situ conversion of benzaldehyde into toluene by using Pd/ND

Benzaldehyde (100 mg), benzylamine (101 mg), and molecular sieves (50 mg, 4 Å) were added to tetrahydrofuran (10 mL) in a round-bottom flask and heated at 60 °C for 150 min. The contents were cooled to 30 °C and then transferred to the autoclave after collecting a sample for GC analysis (10 μL added to 1.5 mL THF). Finally, the catalyst Pd/ND (10 mg) was added to the reactor and it was closed tightly. Air in the reactor was displaced by hydrogen gas, which was inserted at a pressure of 0.6 MPa (three cycles repeated). Care was taken to check the hydrogen level in the surroundings by using a hydrogen gas sensor (Caution: hydrogen is flammable). Finally, the contents were heated at 150 °C for the specified time (Table 4), where the pressure of the autoclave reached a maximum of 1.8 MPa. The contents were cooled to room temperature and the yield of the product was reported by comparison with the standard calibration curve of toluene. Vanillin was also converted by adopting the same procedure.

Acknowledgements

NG thanks the Chinese Academy of Sciences (CAS) for a postdoctoral award. We also thank Jagadeesh Suriyaprakash, Yangming Lin, and Liyun Zhang for extending help during the sample analysis. We thank the Dalian Institute of Chemical Physics (Chinese Academy of Sciences) for providing GCMS facilities.

Keywords: amines · benzonitrile · biomass conversion · lignin · palladium

[1] T. Patra, S. Agasti, Akanksha, D. Maiti, *Chem. Commun.* **2013**, *49*, 69 – 71.
[2] a) Y. Wang, F. S. Guziec, *J. Org. Chem.* **2001**, *66*, 8293 – 8296; b) M. P. Doyle, J. F. Dellaria, Jr., B. Siegfried, S. W. Bishop, *J. Org. Chem.* **1977**, *42*, 3494 – 3498.
[3] S. Liu, X. Fan, X. Yan, X. Du, L. Chen, *Appl. Catal. A* **2011**, *400*, 99 – 103.
[4] a) O. J. Geoffroy, T. A. Morinelli, G. P. Meier, *Tetrahedron Lett.* **2001**, *42*, 5367 – 5369; b) G. A. Doldouras, J. Kollonitsch, *J. Am. Chem. Soc.* **1978**, *100*, 341 – 342.
[5] T. C. Fessard, S. P. Andrews, H. Motoyoshi, E. M. Carreira, *Angew. Chem. Int. Ed.* **2007**, *46*, 9331 – 9334; *Angew. Chem.* **2007**, *119*, 9492 – 9495.
[6] J. Tsuji, K. Ohno, *Tetrahedron Lett.* **1965**, *6*, 3969 – 3971.
[7] T. Iwai, T. Fujihara, Y. Tsuji, *Chem. Commun.* **2008**, 6215 – 6217.
[8] G. Domazetis, B. Tarpey, D. Dolphin, B. R. James, *J. Chem. Soc. Chem. Commun.* **1980**, 939 – 940.
[9] S. Matsubara, Y. Yokota, K. Oshima, *Org. Lett.* **2004**, *6*, 2071 – 2073.
[10] A. Modak, A. Deb, T. Patra, S. Rana, S. Maity, D. Maiti, *Chem. Commun.* **2012**, *48*, 4253 – 4255.
[11] D. Procházková, P. Zámostný, M. Bejblová, L. Červený, J. Čejka, *Appl. Catal. A* **2007**, *332*, 56 – 64.
[12] V. N. Mochalin, O. Shenderova, D. Ho, Y. Gogotsi, *Nat. Nanotechnol.* **2012**, *7*, 11 – 23.
[13] a) A. A. Peristyy, O. N. Fedyanina, B. Paull, P. N. Nesterenko, *J. Chromatogr.* **2014**, *1357*, 68 – 86; b) M. H. Avazkonandeh-Gharavol, S. A. Sajjadi, S. M. Zebarjad, M. Mohammadtaheri, M. Abbasi, M. Alimardani, K. Mossaddegh, *Prog. Org. Coat.* **2013**, *76*, 1258 – 1264; c) E. V. Basiuk, V. A. Basiuk, *J. Nanosci. Nanotechnol.* **2014**, *14*, 644 – 672; d) J. Fan, P. K. Chu, *Small* **2010**, *6*, 2080 – 2098.
[14] G. Li, Z. Tang, *Nanoscale* **2014**, *6*, 3995 – 4011.
[15] a) S. Zhao, H. Yin, L. Du, L. He, K. Zhao, L. Chang, G. Yin, H. Zhao, S. Liu, Z. Tang, *J. Am. Chem. Soc.* **2014**, *136*, 1738 – 1741; b) H. Yin, H. Tang, D. Wang, Y. Gao, Z. Tang, *ACS Nano* **2012**, *6*, 8288 – 8297.
[16] J. Qi, J. Chen, G. Li, S. Li, Y. Gao, Z. Tang, *Energy Environ. Sci.* **2012**, *5*, 8937 – 8941.
[17] L. Zhao, Y. H. Xu, H. Qin, S. Abe, T. Akasaka, T. Chano, F. Watari, T. Kimura, N. Komatsu, X. Chen, *Adv. Funct. Mater.* **2014**, *24*, 5348 – 5357.
[18] Y. Zhao, Y. Wang, X. Cheng, L. Dong, Y. Zhang, J. Zang, *Carbon* **2014**, *67*, 409 – 416.
[19] L. Dong, J. Zang, Y. Wang, H. Pan, Y. Wang, Y. Zhao, J. Su, *J. Electrochem. Soc.* **2014**, *161*, F185 – F191.
[20] O. V. Turova, E. V. Starodubtseva, M. G. Vinogradov, V. I. Sokolov, N. V. Abramova, A. Y. Vul', A. E. Alexenskiy, *Catal. Commun.* **2011**, *12*, 577 – 579.
[21] N. A. Magdalinova, P. A. Kalmykov, M. V. Klyuev, *Pet. Chem.* **2012**, *52*, 299 – 304.
[22] N. A. Magdalinova, P. A. Kalmykov, M. V. Klyuev, *Russ. J. Gen. Chem.* **2014**, *84*, 33 – 39.
[23] O. S. Alekseev, L. V. Nosova, Y. A. Ryndin, *Stud. Surf. Sci. Catal.* **1993**, *75*, 837 – 847.
[24] a) D. S. Su, G. Centi, *J. Energy Chem.* **2013**, *22*, 151 – 173; b) D. S. Su, S. Perathoner, G. Centi, *Chem. Rev.* **2013**, *113*, 5782 – 5816; c) J. Liu, L. Jiang, B. Zhang, J. Jin, D. S. Su, S. Wang, G. Sun, *ACS Catal.* **2014**, *4*, 2998 – 3001.
[25] J. J. W. Bakker, A. G. van der Neut, M. T. Kreutzer, J. A. Moulijn, F. Kapteijn, *J. Catal.* **2010**, *274*, 176 – 191.
[26] S. P. Bawane, S. B. Sawant, *Chem. Eng. J.* **2004**, *103*, 13 – 19.
[27] W. H. Hartung, *J. Am. Chem. Soc.* **1928**, *50*, 3370 – 3374.
[28] A. Demirbaş, *Energy Convers. Manage.* **2001**, *42*, 1357 – 1378.
[29] E. S. Lokteva, E. V. Golubina, S. A. Kachevskii, A. N. Kharlanov, A. V. Erokhin, V. V. Lunin, *Kinet. Catal.* **2011**, *52*, 145 – 155.
[30] E. V. Golubina, E. S. Lokteva, S. A. Kachevsky, *Stud. Surf. Sci. Catal.* **2010**, *175*, 293 – 296.
[31] S. A. Kachevskii, E. V. Golubina, E. S. Lokteva, V. V. Lunin, *Russ. J. Phys. Chem.* **2007**, *81*, 866 – 873.

Received: November 11, 2015
Published online on February 5, 2016